Heliyon 10 (2024) e38376

Contents lists available at ScienceDirect

Heliyon

journal homepage: www.cell.com/heliyon

Research article

Design, synthesis, biological evaluation, kinetic studies and molecular modeling of imidazo-isoxazole derivatives targeting both α-amylase and α-glucosidase inhibitors

Etab AlRashidi [a], Siwar Ghannay [a], Abuzar E.A.E. Albadri [a], Majdi Abid [b], Adel Kadri [c,d,**], Kaiss Aouadi [a,*]

[a] Department of Chemistry, College of Science, Qassim University, Buraidah, 51452, Saudi Arabia
[b] Department of Chemistry, College of Science, Jouf University, P.O. Box 2014, Sakaka, Aljouf, Kingdom of Saudi Arabia
[c] Department of Chemistry, Faculty of Science, Al-Baha University, Al-Baha, 65431, Kingdom of Saudi Arabia
[d] Faculty of Science of Sfax, Department of Chemistry, University of Sfax, B.P. 1171, 3000, Sfax, Tunisia

ARTICLE INFO

Keywords:
Diabetes mellitus
Imidazo-isoxazole derivatives
α-amylase and α-glucosidase inhibition
Enzymatic kinetics
SAR analysis
ADMET
Molecular docking and MD simulations

ABSTRACT

Herein, a novel set of imidazo-isoxazole derivatives containing thiourea and urea scaffolds were synthesized, characterized (^{1}H NMR, ^{13}C NMR, and elemental analysis). These compounds were biologically evaluated for their α-amylase and α-glucosidase inhibitory activity, identifying **5f** as the most active (IC_{50} 26.67 ± 1.25 μM and 39.12 ± 1.83 μM against α-amylase α-glucosidase, respectively), better than the standard, acarbose. Enzymatic kinetic results showed that **5f** and acarbose complete competitive type inhibitors. The structure-activity relationship (SAR) demonstrated that undergoing substitutions on R1 and R2 groups attached to the thiourea/urea moiety chains controlled the activity. Besides, in-silico ADMET study showed that almost title compounds exhibited satisfactory pharmacokinetic properties. In molecular docking study, the top performing compound (**5f**) exhibited higher binding energies (−5.501 and −6.414 kcal/mol, respectively) showing crucial interactions and that snuggly fit in their active site. To shed light on their mechanism of action, molecular dynamic (MD) simulations approach executed at 100 ns duration authenticated the high stability of **5f**-1B2Y and **5f**-3A4A complexes. The results of this investigation disclosed that compound **5f** may serve as a potential lead, accomplished with *in vivo* studies, for the management of diabetes.

1. Introduction

Diabetes mellitus (DM), is a polygenic multifactorial metabolic disorder and an autoimmune and endocrine disease, characterized by high hepatic glucose production or glucose intolerance [1–4]. It has become a critical epidemic with very alarming deaths and morbidity causing the destruction of human safety and health [5,6]. DM can be divided into four main types: Type-1 diabetes (T1DM), type-2 diabetes (T2DM), gestational diabetes mellitus (GDM) and secondary diabetes (SD) as the smallest one [7]. According to the International Diabetes Federation (IDF), 541 million adults (75–79 years) have Impaired Glucose Tolerance (IGT), which is high risk of

* Corresponding author.
** Corresponding author. Department of Chemistry, Faculty of Science, Al-Baha University, Al-Baha, 65431, Kingdom of Saudi Arabia.
E-mail addresses: lukadel@yahoo.fr (A. Kadri), K.AOUADI@qu.edu.sa (K. Aouadi).

https://doi.org/10.1016/j.heliyon.2024.e38376
Received 27 June 2024; Received in revised form 20 September 2024; Accepted 23 September 2024
Available online 24 September 2024

type 2 diabetes, and approximately 643 million people could be living with diabetes by 2030 and increase to 783 million by 2045 [8]. The kingdom of Saudi Arabia was ranked as the third country with a prevalence of 21.4 % and arise in the top 10 countries with the highest reported T2DM diagnosis worldwide [9,10]. α-Glucosidase and α-amylase are two key enzymes playing a pivotal role in the digestion and metabolism of carbohydrates in human body. Their inhibition can control postprandial hyperglycemia and remains as the main therapeutic approach for regulating blood glucose levels via enabling control of postprandial hyperglycemia [11–21]. Commercially and clinically approved inhibitors of these enzymes such as acarbose, miglitol, and voglibose were very associated with unwanted and deleterious side effects including abdominal distension, meteorism, flatulence and diarrhea [22,23]. Thus, searching for novel enzyme inhibitors with potentially less negative side effects becomes a pragmatic inspiration for the management of DM [24].

Nitrogen-based heterocycles are one of the well-known promising scaffolds in drug discovery [25–34]. Compounds containing the (thio)urea function are privileged substructures in medicinal and synthetic chemistry endowed with excellent "druggability" and wide range of various pharmaceutically potencies [2,35–38]. The linearity of this motif and its property as both H-bond acceptor/donor contribute to its bioavailability and hydrophilicity [39,40]. In recent years, chemicals containing the (thio)urea scaffold have been approved as marketable drugs (Fig. 1). Cariprazine, an antipsychotic was approved by US-FDA in 2015 for the treatment of bipolar disorder [41], DPTU (5-dihydroxyboryl-6-propyl-2-thiouracil), an allosteric antagonist, was used as modulator of P2Y1 receptors and a candidate compound for boron neutron capture therapy [42,43], Sorafenib (Nexavar™), an anticancer drug, was marketed by Bayer and Onyx Pharmaceuticals and approved by US-FDA, Thioacetazone was used as antitubercular agent for the treatment Mycobacterium tuberculosis infections [44], Enzalutamide (Xtandi, Astellas Pharma US, Inc.) as a nonsteroidal androgen receptor inhibitor served primary to treat prostate cancer and was approved by on 2023 for non-metastatic castration-sensitive prostate cancer (nmCSPC) [45,46], and Tenovin-1, an inhibitor of the NAD + -dependent protein deacetylases [47].

The anti-diabetic drugs tethered (thio)urea moiety have been also reported as potent α-amylase and α-glucosidase inhibitors [48,49] (Fig. 2).

Since the etiology of DM is multifaceted [50–53], and based on our previous efforts to find dual α-amylase and α-glucosidase inhibitors [1,54–56], the strategy of the conducted work is to incorporate the (thio)urea moiety side chain into imidazo-isoxazole derivatives bearing imino methyl phenol moiety was adopted.

Therefore, the aim of the current contribution was the synthesis of novel imidazo-isoxazole derivatives containing imino methyl phenol and (thio)urea moieties and the study of their α-amylase and α-glucosidase inhibitory activity followed by a kinetic study. Finally, an *in silico* study including ADMET, molecular docking and dynamic simulation was performed by exploring the plausible interactions.

2. Results and discussion

2.1. Chemistry

The reaction sequence illustrated in Scheme 1 is composed of two steps, a 1,3-dipolar cycloaddition (1,3-DC) followed by a condensation. Indeed, the synthesis begins with a 1,3-DC of nitrone **1** with 3-allyl-2-hydroxybenzaldehyde **2** (commercially available from Aldrich) to give the cycloadduct **3**. The synthesized isoxazolidine **3** was engaged in a condensation reaction with (thio)

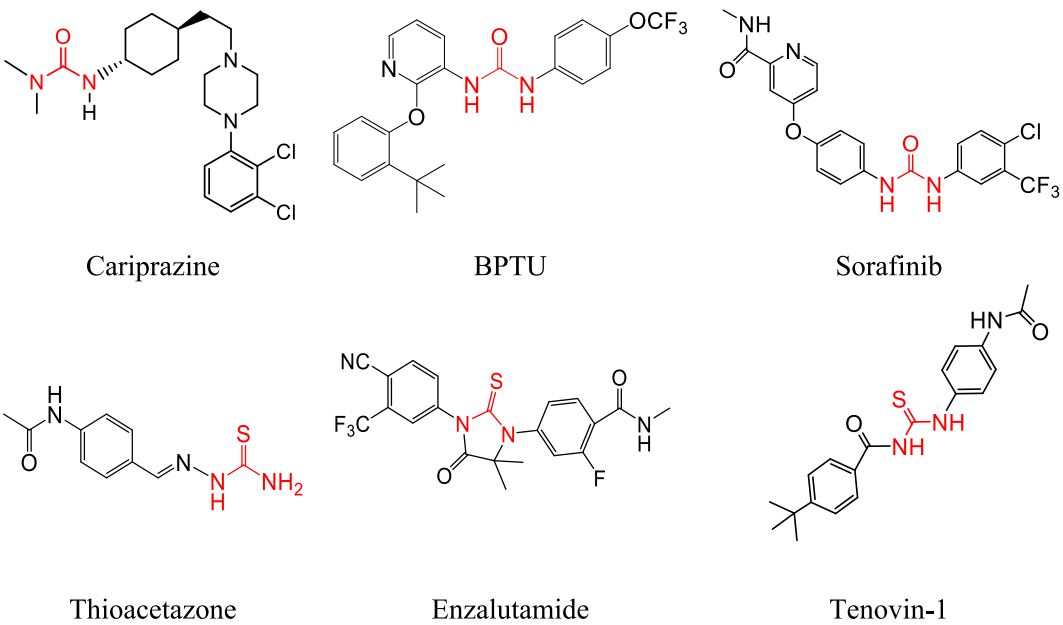

Fig. 1. (Thio)urea marketable drugs.

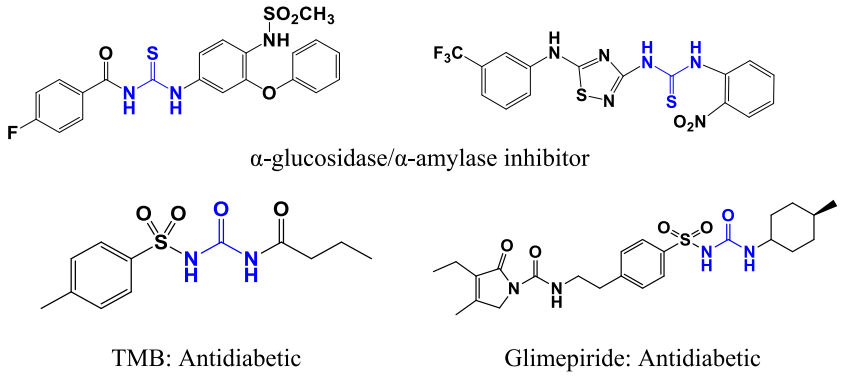

Fig. 2. (Thio)urea α-amylase and α-glucosidase inhibitors.

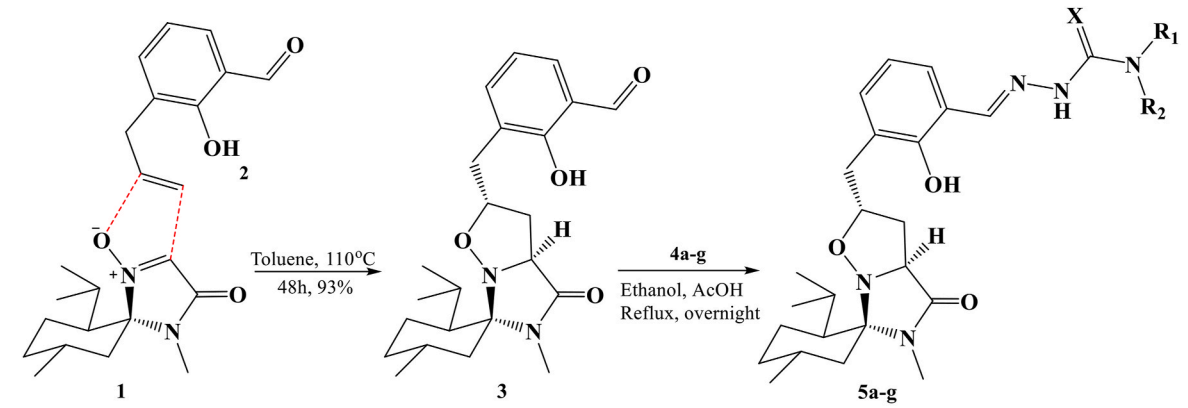

Entry	X	R_1	R_2	Yield
5a	O	Ph	H	84%
5b	S	Ph	H	81%
5c	S	C_2H_5	H	86%
5d	S	CH_3	CH_3	78%
5e	S	H	H	87%
5f	O	H	H	80%
5g	S	CH_3	H	85%

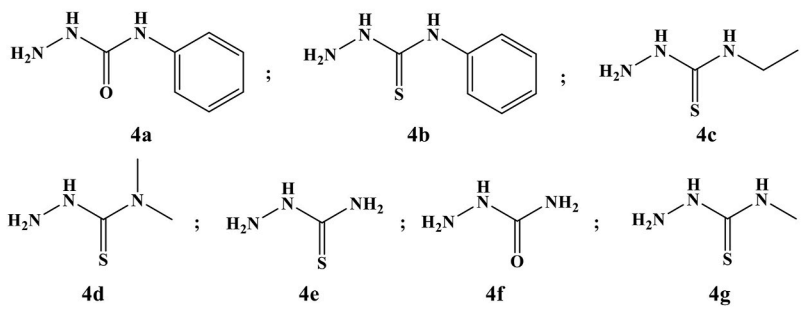

Scheme 1. Synthesis of compounds **5a-g**.

semicarbazide derivatives **4a-g** to access the desired products **5a-g** with good yield.

In 1H NMR spectra of compounds **5a-g**, indicate the presence of H-3, H-4a, H-4b, H-5 and H-6 protons at 3.99, 2.26, 2.64, 4.01 and 2.93 ppm, respectively. ^{13}C NMR spectra of compounds **5a-g** show three signals at 40.3, 66.3 and 89.9 ppm, related to C-4, C-3 and C-5 carbons, respectively. The NMR study of the NOESY 2D spectrum for isoxazolidine **5g** (Fig. 3) showed strong correlations between the H3-H4a, H3-H13 and H4b-H5 protons and no correlation between the H3-H4b protons. These observations indicate that the H3 proton is in the same direction as the H4a and H13 protons and in the opposite direction as the H4b and H5 protons (Fig. 3). These observations are corroborated by the comparison of the coupling constants with data from the literature [57]. Indeed, the coupling constant $J_{3\text{-}4a}$ (*cis*) = 8.4 Hz which is in good agreement with the literature data ($J_{3\text{-}4a}$ (*cis*) ≥ 7.0 Hz) [42]).

2.1.1. In vitro α-amylase and α-glucosidase inhibitory activities and SAR investigation

The synthesized imidazo-isoxazole analogues were subjected to their *in vitro* anti-α-amylase and anti-α-glucosidase activities. Acarbose was used as standard drug and the results were depicted in Table 1. Enzymatic inhibition results of all newly afforded analogues demonstrated a satisfyingly bifunctional potential inhibition effect, in which **5f** as the unsubstituted urea scaffold (Fig. 4) was found to be the most active analog (IC_{50} = 26.67 ± 1.25 μM and 39.12 ± 1.83 μM) with about 11-and 12-fold improvement than

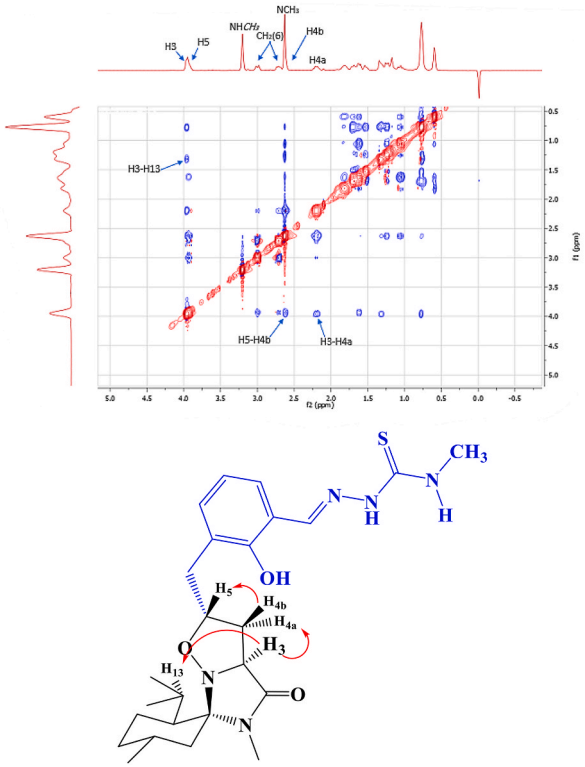

Fig. 3. NOESY 2D NMR of compound **5g**.

Table 1
IC_{50} (μM) of **5a-g**. The means of the same column with a different letter are significantly different ($P < 0.05$). The means of the same column with the same letter are not significantly different ($P > 0.05$).

Entry	X	R_1	R_2	α-Amylase IC_{50} (μM)	α-Glucosidase IC_{50} (μM)
5a	O	Ph	H	151.22 ± 7.4^{e}	262.5 ± 12.23^{f}
5b	S	Ph	H	197.95 ± 9.5^{f}	286.2 ± 13.5^{f}
5c	S	C_2H_5	H	73.08 ± 3.31^{b}	202.6 ± 10.02^{e}
5d	S	CH_3	CH_3	58.76 ± 2.22^{c}	98.61 ± 4.35^{c}
5e	S	H	H	33.88 ± 1.09^{b}	49.31 ± 2.19^{b}
5f	O	H	H	26.67 ± 1.25^{a}	39.12 ± 1.83^{a}
5g	S	CH_3	H	64.17 ± 3.15^{c}	157.8 ± 7.09^{d}
Acarbose	–			296.6 ± 0.825	780.4 ± 0.346

acarbose, respectively. Urea derivatives (**5a** and **5f**) were found to be more potent than the corresponding thiourea one (**5b** and **5e**). The replacement of a hydrogen attached to the proximal NH of the thiourea moiety by an alkyl group loses the inhibitory effect. This reduction was more pronounced upon changing the methyl group in **5g** ($IC_{50} = 64.17 \pm 3.15$ μM and 157.8 ± 7.09 μM) by an ethyl one in **5c** ($IC_{50} = 73.08 \pm 3.31$ μM and 202.6 ± 10.02 μM) suggesting that increased the long chain alkyl group abolishes the activity. Conversely, upon replacing the second hydrogen atom in -NH_2 (**5g**), by another methyl group (**5d**), enhances tremendously the enzymatic inhibition activity ($IC_{50} = 58.76 \pm 2.22$ μM and 98.61 ± 4.35 μM). A drop in the inhibitory effect was dramatically observed when the hydrogen atom attached to the proximal NH of the thiourea/urea core was substituted by a hydrophobic group such as phenyl (**5a** and **5b**).

2.2. Enzymatic kinetic studies

2.2.1. Mode of α-amylase inhibition by 5f and acarbose

To gain further insight into the inhibition mechanism of **5f** and acarbose on α-amylase. Both Lineweaver–Burk plots and secondary re-plot of Lineweaver–Burk plots were used to determine the inhibition mode and the value of the inhibition constant, Ki. Our results (Fig. 5, A and C) indicate that the maximum rate V_{max} was unchanged however the Michaelis constant, K_m gradually increased meaning that **5f** displayed a competitive inhibition against α-amylase and acarbose. Ki values (Fig. 5, B and D) of compound **5f** and acarbose were 24.88 μM and 293.63 μM, respectively. Thus, our finding revealed that **5f** competes with the substrate for better binding

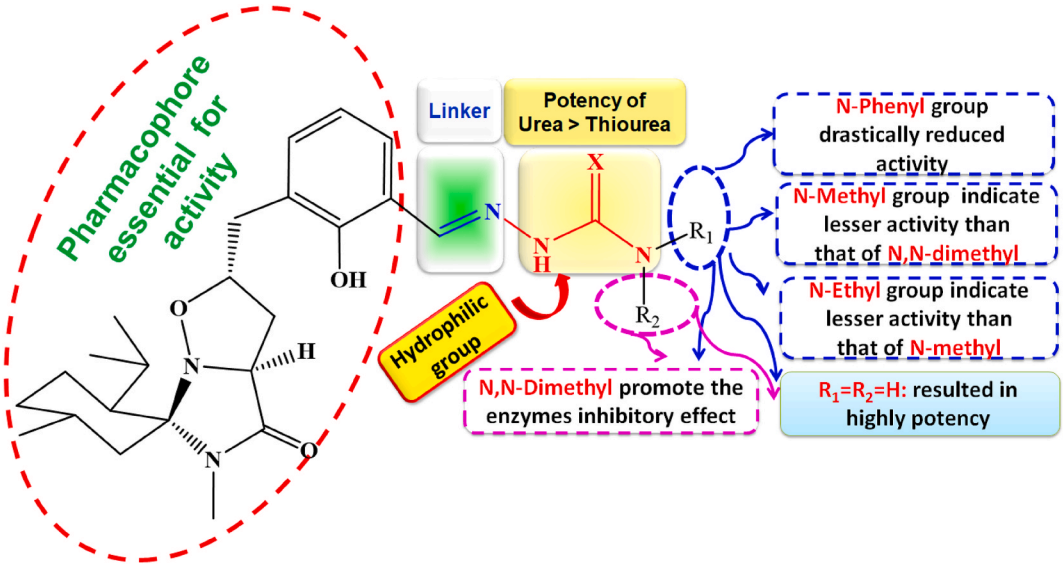

Fig. 4. SAR of the synthesized compounds.

to the active site of α-amylase.

2.2.2. *Mode of α-glucosidase inhibition by 5f and acarbose*

An inhibition kinetics study was explored to understand the inhibition mechanism of **5f** and acarbose on α-glucosidase. Graphs of various concentrations of inhibitor, were drawn via the Lineweaver–Burk plot (Fig. 6, A and C), indicated that Vmax values remained unaffected, however the Km values increased to overcome the inhibitory effect of the competitor. The observed inhibition type revealed that **5f** and acarbose bind to the active site on the enzyme and compete with the substrate for binding to the active site. The slope of each line in the Lineweaver–Burk plots was plotted towards into various concentrations of **5f** (Fig. 6, B) and acarbose (Fig. 6, D) to elucidate the inhibition constant Ki, which were found to be 36.98 μM and 750.96 μM, respectively.

2.2.2.1. Acute oral toxicity. The most active compound **5f** was subjected for its acute oral toxicity analysis towards three female mice [54]. Obtained *in vivo* data indicated that **5f** present no toxicity up to 1000 mg/kg b.w., without any significant adverse effects or mortality, however, at a dose of 1600 mg/kg b.w., only one mouse was survived, suggesting that this concentration provoke mortality. Thus, 50 mg/kg.b.w. was selected as the dose for the further studies.

2.3. *Molecular modeling*

2.3.1. *ADMET profiling results*

The pharmacokinetic profile of the newly synthesized analogues was performed using pkCSM and Swiss ADME descriptor algorithm procedures to get insights into their specific effectiveness in the body [58–61]. Druglikness based on how a lead molecule is well absorbed, distributed, broken down, and eliminated remains a crucial step in drug design and lead optimization for high bioactivity and low toxicity [62–65]. As summarized in Table 2, based on pkCSM analysis, we can assume that all examined analogues are P-glycoprotein inhibitor, exhibiting good absorption properties with acceptable water solubility values, Caco2 permeability level higher than 0.9 and very potent gastrointestinal absorption in human (75.14 %–94.437 %) meaning their easier behavior to cross different biological membranes. Our prepared compounds can reach skin permeability (log Kp) values ranging from −3.148 to −2.739. Regarding their distribution properties, the predicted data showed good volume of distribution at steady state expressed by VDss, acceptable unbound fraction, and moderate blood-brain barrier (BBB) and central nervous system (CNS) permeability. The parameters related to metabolism mode showed that the investigated compounds could not inhibit all tested cytochrome P450 enzymes, that catalyze metabolism, mainly those of CYP2D6 and CYP3A4 enzymes implicated in the process of more than 60 % of drugs, and therefore suggest that they are lacking of any toxic effect. Excretion parameters including total clearance (hepatic and renal) and renal OCT2 substrate were also predicted. The prediction of the toxicity profile via different parameters such as AMES (Mutagenicity), hERG I and II inhibitor, and skin sensitization demonstrated that all compounds did not present any particular toxicity and could be safe for further investigation.

The *in-silico* analysis of the subsequent compounds was also carried out using Swisss ADME software. To be a successful oral candidate drug, the bioavailability radar (Fig. 7) of the title compounds was assessed. All analogues fall entirely the pink area suggesting that they are suitable for better bioavailability.

The prediction of brain permeability and gastrointestinal absorption is an essential step in drug development stage to elucidate the

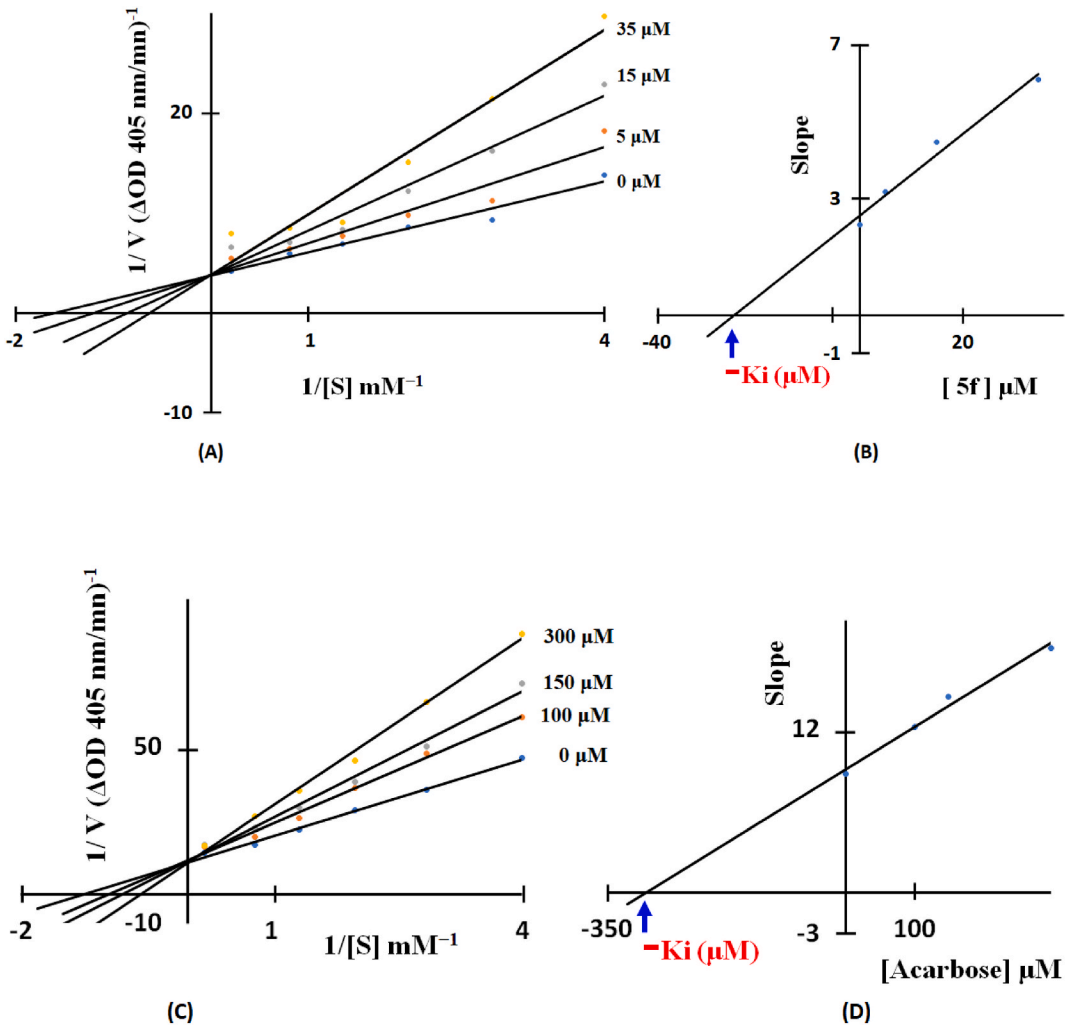

Fig. 5. Lineweaver-Burk plots for the inhibition of α-amylase by **5f** (**A**) and acarbose (**C**), respectively. (**B**) and (**D**) are respectively the secondary plot between the slopes of each line on Lineweaver–Burk plot and different concentrations of compound **5f** and acarbose.

pharmacology and bioavailability of a candidate molecule. As shown in Fig. 8, all the synthesized compounds exhibit gastrointestinal absorption but none of them able to passively across the blood-brain barrier.

2.3.2. Molecular docking results

The molecular docking study was performed to evaluate the binding affinity of the synthesized compounds **5a-g** towards human pancreatic α-amylase (PDB ID: 1B2Y) and α-glucosidase (PDB ID: 3A4A), with the goal of assessing their antidiabetic potential (Table 3).

The docking scores, expressed in kcal/mol, provide a measure of the binding energy between each compound and the target enzymes. A more negative docking score indicates a stronger binding interaction between the compound and the enzyme. For α-amylase, the docking scores ranged from −4.209 kcal/mol (**5g**) to −6.724 kcal/mol (**5b**). The top three compounds with the most favorable docking scores were **5b** (−6.724 kcal/mol), **5f** (−5.501 kcal/mol), and **5c** (−4.932 kcal/mol). These compounds may have a higher potential to inhibit α-amylase activity, leading to reduced carbohydrate digestion and glucose absorption. For α-glucosidase, the docking scores ranged from −4.232 kcal/mol (**5a**) to −6.487 kcal/mol (**5e**) (Table 3). The top three compounds with the most favorable docking scores were **5e** (−6.487 kcal/mol), **5f** (−6.414 kcal/mol), and **5d** (−5.54 kcal/mol).

The SAR analysis revealed that urea derivatives, particularly **5a** and **5f**, exhibited stronger inhibitory effects against both α-amylase and α-glucosidase compared to their thiourea counterparts, **5b** and **5e**. This was reflected in the docking scores, where the urea derivatives consistently showed better binding affinities. Additionally, modifying the -NH_2 group by substituting one hydrogen atom with a methyl group, as seen in compound **5d**, significantly enhances activity, particularly against α-glucosidase, suggesting that small alkyl groups can optimize enzyme binding. Conversely, replacing the methyl group with a longer ethyl chain, as in compound **5c**, decreases activity, likely due to steric hindrance affecting the binding interaction. Notably, compound containing nitrone moiety, **5f**

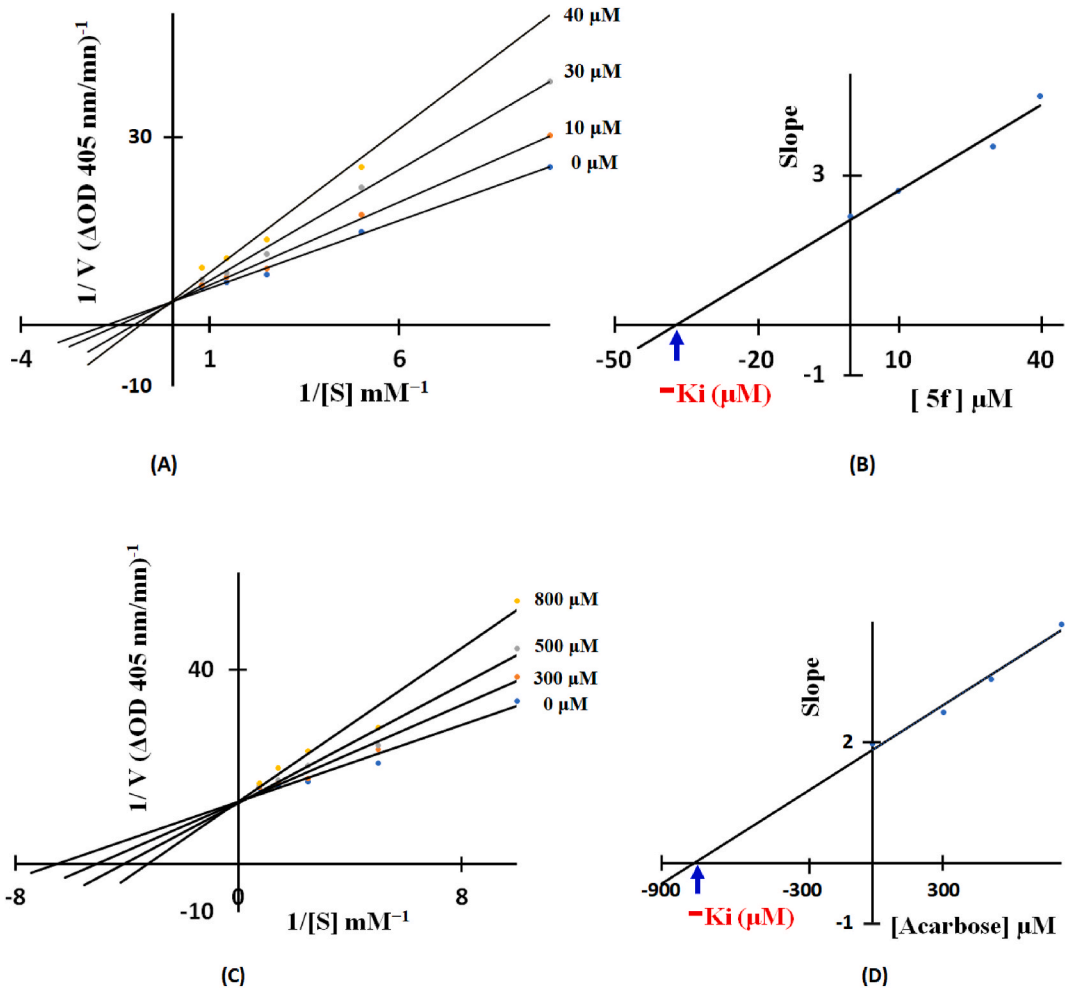

Fig. 6. Lineweaver-Burk plots for the inhibition of α-glucosidase by **5f** (**A**) and acarbose (**C**), respectively. (**B**) and (**D**) are respectively the secondary plot between the slopes of each line on Lineweaver–Burk plot and different concentrations of compound **5f** and acarbose.

exhibited promising binding interactions with both α-amylase and α-glucosidase, suggesting that they may be potential leads for antidiabetic therapy. The nitrone moiety, which features a C=N^+–O^- bond, introduces a unique electronic environment that could modulate the interaction with the active sites of α-amylase and α-glucosidase. This group might contribute to the stabilization of the enzyme-inhibitor complex through either direct hydrogen bonding or by influencing the conformation of adjacent functional groups, such as the terminal urea group. Additionally, the electron-withdrawing nature of the nitrone group could potentially increase the electrophilicity of nearby carbon atoms, facilitating more robust interactions with nucleophilic residues in the enzyme active sites [66, 67]. In compound **5f**, the nitrone group could be enhancing the binding interactions by positioning the terminal urea group favorably within the active sites of α-amylase and α-glucosidase. The nitrone group's influence might also extend to improving the overall molecular rigidity, leading to a better fit within the enzyme's binding pocket, which is consistent with the observed IC_{50} values of 26.6 µM and 39.12 µM for α-amylase and α-glucosidase, respectively.

Notably, compound **5f**, which contains a terminal urea group, exhibited promising binding interactions with both α-amylase and α-glucosidase, suggesting its potential as a lead compound for antidiabetic therapy. The docking studies revealed that in the α-amylase protein, **5f** forms three hydrogen bonds: one from the terminal urea amino group with Asp300 and Asp197, and another from the polar hydroxyl group with His305 (Fig. 8). These interactions are comparable to those observed with the standard inhibitor Acarbose, indicating **5f**'s potential to inhibit this enzyme effectively [68].

Similarly, in the α-glucosidase protein, **5f** establishes two hydrogen bonds: the amino group interacts with Asp215, and the hydroxyl group interacts with Glu411. The comparable binding approach and docking scores of **5f** suggest that it can potentially inhibit α-glucosidase, contributing to its dual inhibitory effect on carbohydrate digestion and glucose absorption.

2.3.3. Molecular dynamic simulation results

Molecular dynamics simulations were employed to assess the stability of ligand-enzyme complexes. This approach provided

Table 2
ADMET properties of the synthesized compounds using pkCSM.

Entry	5a	5b	5c	5d	5e	5f	5g	Reference
Absorption								
Water solubility	−4.219	−4.23	−4.712	−4.76	−4.481	−4.12	−4.622	–
Caco2 permeability	1.481	1.061	0.974	0.982	1.116	1.062	0.983	*>0.9*
Intestinal absorption (human)	85.545	91.678	94.018	94.228	75.14	78.637	94.437	*<30 % is poorly*
Skin Permeability (log Kp)	−2.739	−2.739	−3.052	−3.083	−3.121	−3.148	−3.107	*>-2.5 is low*
P-glycoprotein inhibitor	Yes	Yes	Yes	Yes	Yes	Yes	Yes	*No*
Distribution								
VDss (human)	0.227	0.353	−0.003	−0.003	−0.1	−0.208	−0.046	*Low is < -0.15, High is > 0.45*
Fraction unbound (human)	0.043	0.038	0.113	0.108	0.144	0.154	0.128	-
BBB permeability	−1.13	−1.013	−1.004	−0.954	−0.972	−1.088	−0.953	*Poorly is < -1, High is > 0.3*
CNS permeability	−2.168	−2.062	−2.56	−2.463	−2.629	−2.74	−2.552	*Penetrate is > -2, Unable is < -3*
Metabolism								
CYP1A2 inhibitior	–	–	–	–	–	–	–	–
CYP2C19 inhibitior	–	–	–	–	–	–	–	–
CYP2C9 inhibitior	–	–	–	–	–	–	–	–
CYP2D6 inhibitior	–	–	–	–	–	–	–	–
CYP3A4 inhibitior	–	+	–	–	–	–	–	–
Excretion								
Total Clearance	0.355	−0.01	0.09	0.313	0.028	0.646	0.135	–
Renal OCT2 substrate	No	No	No	No	No	No	No	–
Toxicity								
AMES toxicity	No	No	No	No	No	No	No	*No*
Max. tolerated dose (human)	−0.611	−0.571	−1.02	−1.063	−0.968	−0.935	−1.019	*Low is ≤ 0.477, High is > 0.477*
hERG I inhibitor	No	No	No	No	No	No	No	*No*
hERG II inhibitor	Yes	Yes	Yes	Yes	Yes	Yes	Yes	*No*
Oral Rat Acute Toxicity (LD50)	3.229	3.212	3.243	3.245	3.118	3.132	3.188	-
Oral Rat Chronic Toxicity (LOAEL)	0.522	0.551	0.484	0.504	0.723	0.756	0.622	-
Hepatotoxicity/Skin Sensitization	Yes	Yes	Yes	Yes	Yes	Yes	Yes	*No*
T.Pyriformis toxicity	No	No	No	No	No	No	No	
Minnow toxicity	0.304	0.308	0.388	0.392	0.392	0.361	0.394	

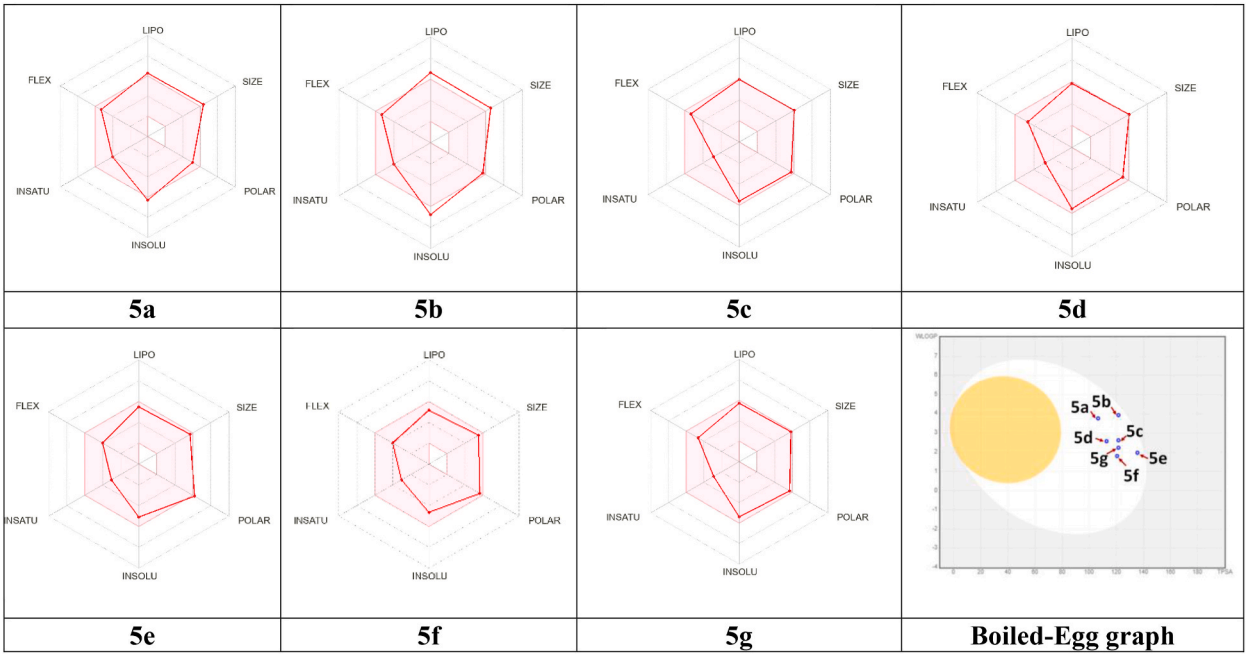

Fig. 7. Radar plot and Boiled-Egg graph of the synthesized analogues **5a-g**.

valuable insights into the dynamic behavior of the compound under investigation, considering long trajectories in a solvated medium and physiological salt concentrations. Following a 200 ns simulation cycle for each complex, analysis was performed on parameters such as RMSD, RMSF, and H-bonds.

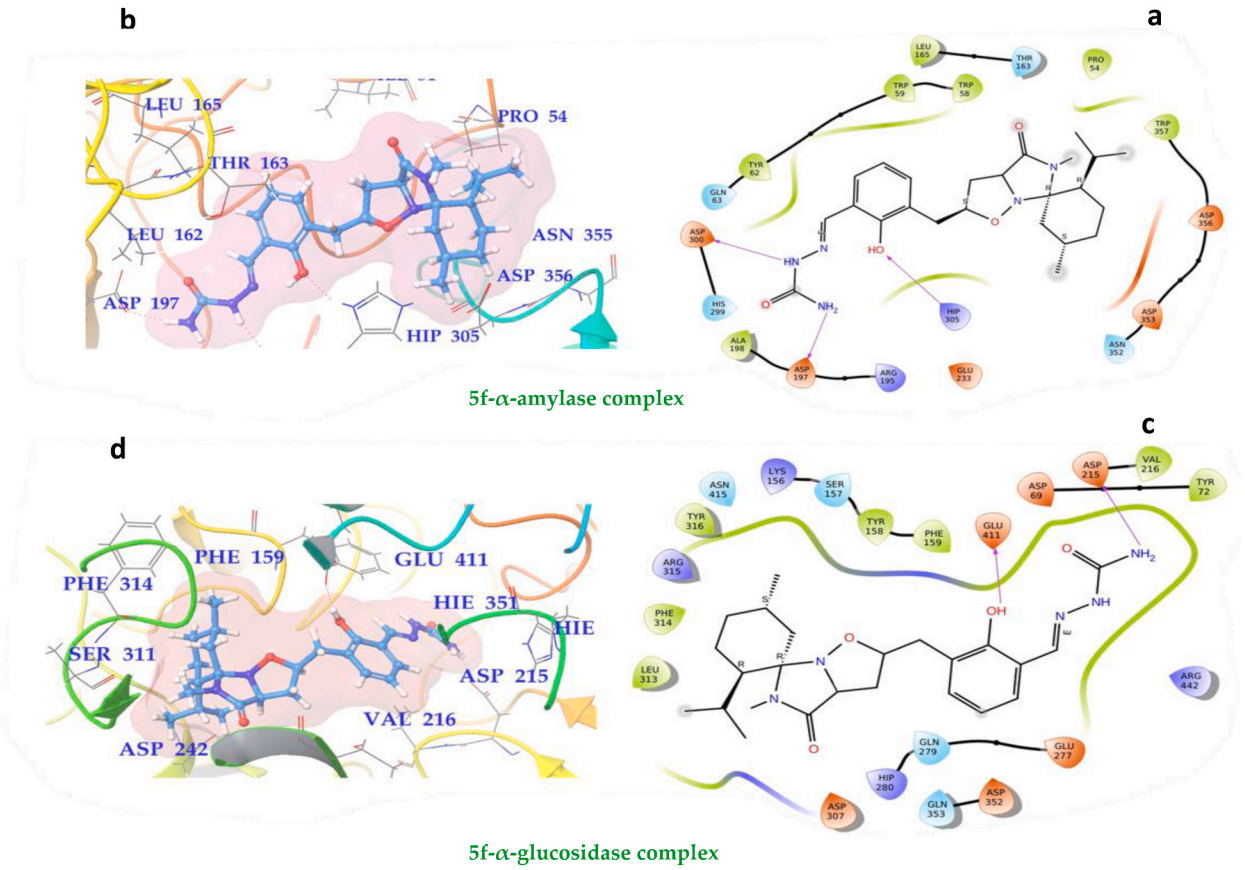

Fig. 8. 2D (a and c) and 3D (b and d) Binding poses of promising compound **5f** in the active of site α-amylase enzyme (PDB ID: 1B2Y) and α-glucosidase enzyme (PDB ID: 3A4A) (*Hydrogen bond interaction is shown by pink arrow line*).

Table 3
Docking score of synthesized compounds against α-amylase and α-glucosidase enzyme.

Compounds	Docking score in Kcal/mol	
	α-Amylase (PDB ID: 1B2Y)	α-Glucosidase (PDB ID: 3A4A)
5a	−4.33	−4.232
5b	−6.724	−4.321
5c	−4.932	−4.325
5d	−4.857	−5.54
5e	−4.853	−6.487
5f	−5.501	−6.414
5g	−4.209	−4.833
Acarbose	−9.020	−8.215

- **Root mean square deviation (RMSD)**

The RMSD trajectories of **5f**-protein complexes over a 200 ns simulation were illustrated in Fig. 9, providing valuable insights into their dynamic behavior. Both complexes exhibit acceptable stability, with RMSD values within the 1-3Å range. The **5f**-1B2Y Complex starts with a higher RMSD, around 1.5 Å, and experiences a peak reaching close to 2.0 Å before stabilizing slightly below 1.5 Å toward the end of the simulation. In contrast, the **5f**-3A4A Complex starts from a lower RMSD, close to 1.0 Å, remains more consistent with fewer fluctuations, and ends with an RMSD around 1.3 Å. Although both complexes can adopt similar conformations at certain points during the simulation, as indicated by their minimum RMSD values of 0.94 Å and 0.82 Å, respectively, the **5f**-3A4A complex appears more stable and less prone to large conformational changes compared to the **5f** -1B2Y complex, given its lower average RMSD value and smaller range of RMSD fluctuations (Fig. 9A**).**

- **Root mean square fluctuation (RMSF)**

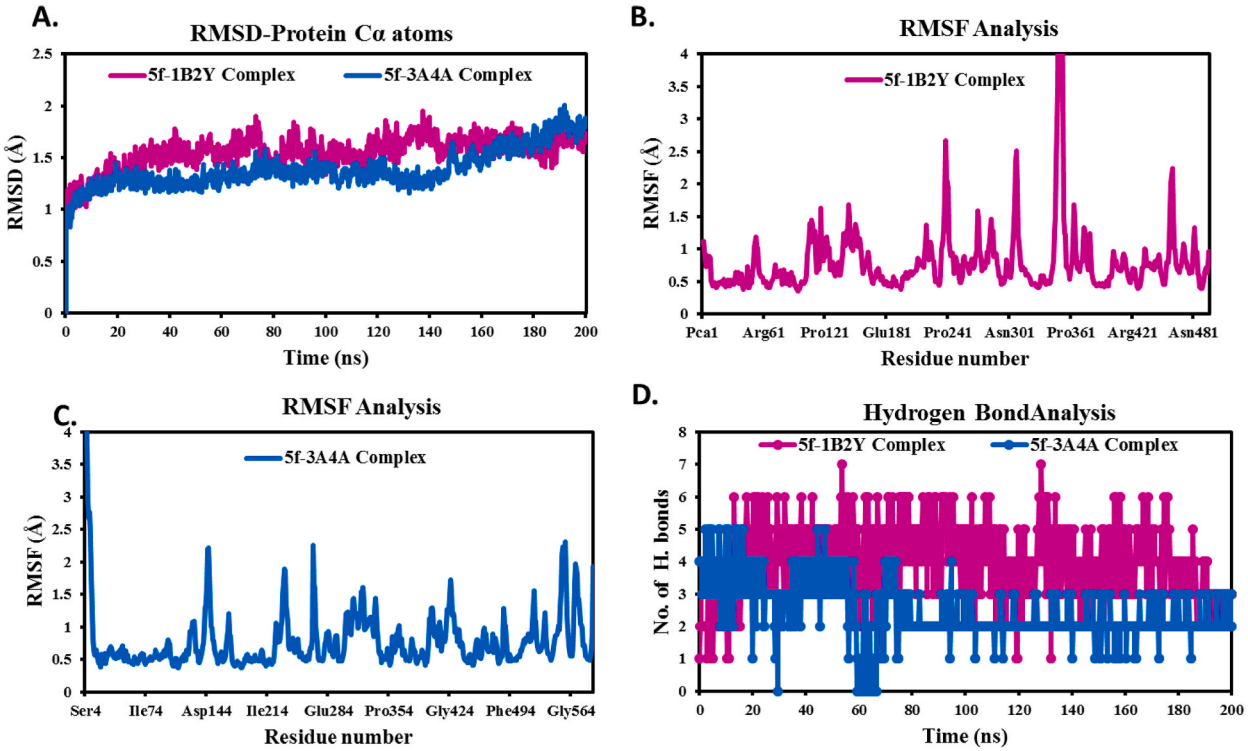

Fig. 9. A. Time-dependent RMSD of Cα atoms of 5f-1B2Y and 5f-3A4A Complexes; **B**. RMSF of individual amino acids of Cα atoms of 5f-1B2Y complex; **C**. RMSF of individual amino acids of Cα atoms of 5f-3A4A complex; **D**. Time-dependent Hydrogen bond analysis of 5f-1B2Y and 5f-3A4A complexes.

RMSF analysis quantifies the atomic deviations from their average positions over time, providing insights into residue-level flexibility and mobility within biomolecular systems. Higher RMSF values signify increased flexibility or mobility, while lower values indicate relatively rigid or stable regions. The resulting flexibility profile is typically visualized through plots of RMSF values against residue number or atom index, offering a graphical representation of the molecule's dynamic behavior. The minimum RMSF values for both complexes are relatively close, with **5f** -1B2Y at 0.36 Å and **5f** -3A4A at 0.37 Å, indicating that both complexes have similarly rigid regions (Table 4). The average RMSF values also indicate a slightly higher flexibility in **5f** -1B2Y, with an average value of 0.83 Å compared to 0.78 Å in **5f** -3A4A. In the **5f** -1B2Y complex, the RMSF analysis reveals that residues Asp353, Phe348, Gln349, Asn352, Asn350, and Gly351

Exhibit high flexibility with RMSF values of 3.34 Å, 3.48 Å, 5.55 Å, 6.19 Å, 8.00 Å, and 8.15 Å, respectively, indicating increased mobility and potential conformational changes, although these residues are not involved in ligand binding. In this complex, 20 amino acids interact with the ligand, with the top interacting residues being Arg195, Arg337, Glu233, Thr254, Gln63, His101, Tyr62, Asp197, Trp58, Trp59, Val234, Asn301, Leu165, His299, Asp300, Asn298, Phe256, Leu162, Thr163, and Ile235, which exhibited RMSF values

Table 4
The Minimum, maximum and average values of different parameters, RMSD, RMSF, RGyr, and Hydrogen Bonding of studied complex and control complex.

	5f -1B2Y Complex	5f -3A4A Complex
Root-mean-square deviation Å (RMSD)		
Minimum	0.94	0.82
Maximum	1.94	2.10
Average	1.55	1.39
Root-mean-square fluctuation Å (RMSF)		
Minimum	0.36	0.37
Maximum	8.16	5.59
Average	0.83	0.78
Hydrogen Bonding		
Minimum	1.0	1.0
Maximum	7.0	5.0
Average	3.9	2.5

ranging from 0.4 to 1.0 Å (Fig. 9B). In the **5f** -3A4A complex, 27 amino acids including Asp69, Tyr72, His112, Tyr158, Phe159, Phe178, Gln182, Asp215, Val216, Leu246, Gln279, His280, Phe303, Ser304, Asp307, Thr310, Ser311, Pro312, Leu313, Phe314, Arg315, Tyr316, Asp352, Glu411, Asn415, Arg442, and Arg446 have RMSF values ranging from 0.4 to 1.44 Å, with higher values observed in the C-terminal residues (Fig. 9C). The observed low RMSF values of the binding site residues demonstrate the stability of compound **5f** binding to the 1B2Y and 3A4A proteins, underscoring their potential as effective inhibitors.

- **Hydrogen bonds Analysis**

Hydrogen bond analysis is a crucial aspect of molecular dynamics simulations, providing valuable insights into the structural integrity and interactions of biomolecules. In the context of protein-ligand interactions, hydrogen bonds play a vital role in determining the specificity and strength of these interactions. The hydrogen bond analysis of the **5f** -protein complexes revealed interesting trends. In both complexes, the minimum number of hydrogen bonds formed in both complexes is 1.0, indicating that at least one hydrogen bond is consistently present throughout the simulation. However, the maximum number of hydrogen bonds differs significantly between the two complexes (Fig. 9D). The **5f** -1B2Y complex forms up to 7.0 hydrogen bonds, whereas the **5f** -3A4A complex forms up to 5.0 hydrogen bonds. This suggests that the **5f** -1B2Y complex has a greater potential for forming multiple hydrogen bonds with the ligand, which could contribute to its increased binding affinity. The average number of hydrogen bonds formed in each complex also provides valuable information. The **5f** -1B2Y complex maintains an average of 3.9 hydrogen bonds, while the **5f** -3A4A complex maintains an average of 2.5 hydrogen bonds. This indicates that the **5f** -1B2Y complex exhibits a more consistent and stable pattern of hydrogen bonding with the ligand, which could be essential for its biological activity. Overall, the hydrogen bond analysis suggests that the **5f** -1B2Y complex has a more extensive and stable network of hydrogen bonds with the ligand, potentially contributing to its increased binding affinity and biological activity compared to the **5f** -3A4A complex.

3. Materials and methods

3.1. α-Amylase and α-glucosidase inhibition Assays

The enzymatic inhibition activity of the synthesized hits towards human pancreatic α-amylase and human lysosomal acid-α-glucosidase enzymes was carried out referring to our previously methods with minor modifications [69,70]. Acarbose was used as standard. All experiments were performed in triplicates.

3.2. Enzymatic kinetic Assays

The inhibition mode of the most potent inhibitor **5f** as identified with its lowest IC_{50} value and the standard drug acarbose was selected for kinetic analysis against α-amylase and α-glucosidase enzymes. A 20 μL of enzyme solution was incubated for 15 min at 30 °C using different concentrations of the inhibitor 5d against α-amylase (0, 5, 15 and 35 μM) and α-glucosidase (0, 10, 30, and 40 μM). The kinetics was started by adding concentrations of each substrate (starch) in the range 0.25–5 mM, and (*p*-nitrophenyl-α-D-glucopyranoside, *P*-NPg) in the range 0.1–1.3 mM, respectively. according to some previously methods, with minor modification [1, 54].

3.3. Molecular docking and molecular dynamic simulation (MD) studies

A molecular docking study was conducted to better understand the molecular basis of the interaction of newly synthesized derivative with anti-diabetic protein receptors. The crystalline structures of the α-amylase enzyme (PDB: 2QV4) and α-glucosidase enzyme (PDB: 3W37) were obtained from PDB (Protein Data Bank). Molecular docking was performed using Schrödinger glide, and MD simulation was performed using Schrödinger's Desmond program [57].

3.4. ADMET property predictions

ADMET profile was determined using both online servers, http://www.swissadme.ch/and https://biosig.lab.uq.edu.au/pkcsm/ accessed on April 22, 2024.

4. Conclusions

In summary, seven new imidazo-isoxazole-based compounds were designed and successfully synthesized and characterized through various spectroscopic techniques. The obtained structures **5a–g**, were tested for their inhibitory activity against α-amylase and α-glucosidase enzymes. The most potent inhibitory activity towards both enzymes was found by **5f** which is about 11 and 20-folds higher than the standard drug, acarbose. Also, oral acute toxicity experiments revealed that 5f was found to be non-toxic and safe at the level concentration. Enzyme inhibition kinetics showed that **5f** competitively inhibit the enzyme and acarbose to form an enzyme inhibitor complex. Conducted SAR study proved the implication of the thio(urea) moiety as a molecular hybrid and the substituents at -R1 and -R2 groups to direct the activity. In addition, ADMET prediction revealed that all synthesized compounds were well drug-likeness with good range of pharmacokinetic properties and are safe. Additionally, molecular docking and MD simulation

analysis demonstrate the high binding and stability of **5f** inside the active site of 1B2Y and 3A4A proteins, confirming the experimental findings. The *in vitro* results are well correlated with the *in-silico* studies. To validate the cheminformatic studies, further *in vivo* experiments will be performed.

Data availability statement

Data included in article/supplementary material is referenced in the article.

CRediT authorship contribution statement

Etab AlRashidi: Visualization, Software, Formal analysis. **Siwar Ghannay:** Writing – review & editing, Writing – original draft, Visualization, Validation, Investigation, Conceptualization. **Abuzar E.A.E. Albadri:** Formal analysis. **Majdi Abid:** Validation, Formal analysis. **Adel Kadri:** Writing – review & editing, Writing – original draft, Visualization, Validation, Investigation, Conceptualization. **Kaiss Aouadi:** Writing – review & editing, Writing – original draft, Validation, Supervision, Methodology, Investigation, Conceptualization.

Declaration of competing interest

The authors declare that they have no known competing financial interests or personal relationships that could have appeared to influence the work reported in this paper.

Appendix A. Supplementary data

Supplementary data to this article can be found online at https://doi.org/10.1016/j.heliyon.2024.e38376.

References

[1] S. Ghannay, B.S. Aldhafeeri, I. Ahmad, E.A.E.A. Albadri, H. Patel, A. Kadri, K. Aouadi, Identification of dual-target isoxazolidine-isatin hybrids with antidiabetic potential: design, synthesis, *in vitro* and multiscale molecular modeling approaches, Heliyon 10 (2024) E25911.
[2] W. Widowati, L. Darsono, H.S. Utomo, A.H. Nur Sabrina, M.R. Natariza, A.C.V. Tarigan, N.W. Waluyo, A.M. Gleyriena, B.H. Siahaan, R. Oktaviani, Antidiabetic and hepatoprotection effect of butterfly pea flower (Clitoria ternatea L.) through antioxidant, anti-inflammatory, lower LDH, ACP, AST, and ALT on diabetes mellitus and dyslipidemia rat, Helyion 10 (2024) E29812.
[3] J.S. Yun, S.H. Jung, M. Shivakumar, et al., Polygenic risk for type 2 diabetes, lifestyle, metabolic health, and cardiovascular disease: a prospective UK Biobank study, Cardiovasc. Diabetol. 21 (2022) 131.
[4] W. Jiang, K. Ding, W. Huang, F. Xu, M. Lei, R. Yue, Potential effects of bisphenol A on diabetes mellitus and its chronic complications: a narrative review, Helyion 9 (2023) E16340.
[5] M.G. Yu, D. Gordin, J. Fu, K. Park, Q. Li, G.L. King, Protective factors and the pathogenesis of complications in diabetes, Endocr. Rev. 45 (2024) 227–252.
[6] C. Qu, X. Tan, Q. Hu, J. Tang, Y. Wang, C. He, Z. He, B. Li, X. Fu, Q. Du, A systematic review of astragaloside IV effects on animal models of diabetes mellitus and its complications, Helyion 10 (2024) E26863.
[7] M.Z. Banday, A.S. Sameer, S. Nissar, Pathophysiology of diabetes: an overview, Avicenna J. Med. 10 (2020) 174–188.
[8] https://idf.org/about-diabetes/diabetes-facts-figures/(assessed on 4/9/2024).
[9] M. Jebril, X. Liu, Z. Shi, M. Mazidi, A. Altaher, Y. Wang, Prevalence of type 2 diabetes and its association with added sugar intake in citizens and refugees aged 40 or older in the gaza strip, Palestine, Int. J. Environ. Res. Public Health 17 (2020) 8594.
[10] K.S. Alwadeai, S.A. Alhammad, Prevalence of type 2 diabetes mellitus and related factors among the general adult population in Saudi Arabia between 2016-2022: a systematic review and meta-analysis of the cross-sectional studies, Medicine (Baltim.) 16 (2023) e34021.
[11] A.P. Kalinovskii, O.V. Sintsova, I.N. Gladkikh, E.V. Leychenko, Natural inhibitors of mammalian α-amylases as promising drugs for the treatment of metabolic diseases, Int. J. Mol. Sci. 24 (2023) 16514.
[12] S. Malik, M.A. Lodhi, S. Ayaz, Z. Ullah, Unlocking potential diabetes therapeutics: insights into alpha-glucosidase inhibition, J. Mol. Liq. 400 (2024) 124572.
[13] M. Li, H. Li, X. Min, J. Sun, B. Liang, L. Xu, J. Li, S.H. Wang, X. Xu, Identification of 1,3,4-thiadiazolyl-containing thiazolidine-2,4-dione derivatives as novel PTP1B inhibitors with antidiabetic activity, J. Med. Chem. 67 (2024) 8406–8419.
[14] C. Hu, B. Liang, J. Sun, J. Li, Z. Xiong, S.H. Wang, X. Xuetao, Synthesis and biological evaluation of indole derivatives containing thiazolidine-2,4-dione as α-glucosidase inhibitors with antidiabetic activity, Eur. J. Med. Chem. 264 (2024) 115957.
[15] B. Liang, D. Xiao, S.H. Wang, X. Xu, Novel thiosemicarbazide-based β-carboline derivatives as α-glucosidase inhibitors: synthesis and biological evaluation, Eur. J. Med. Chem. 275 (2024) 116595.
[16] M. Li, J. Sun, B. Liang, X. Min, J. Hu, R. Wu, X. Xu, Thiazolidine-2,4-dione derivatives as potential α-glucosidase inhibitors: synthesis, inhibitory activity, binding interaction and hypoglycemic activity, Bioorg. Chem. 144 (2024) 107177.
[17] M. Feng, B. Liang, J. Sun, X. Min, S. Wang, Y. Lu, et al., Synthesis, anti-α- glucosidase activity, inhibition interaction, and anti-diabetic activity of novel cryptolepine derivatives, J. Mol. Struct. 1310 (2024) 138311.
[18] J. Lin, D. Xiao, L. Lu, B. Liang, Z. Xiong, X. Xu, New β-carboline derivatives as potential α-glucosidase inhibitor: synthesis and biological activity evaluation, J. Mol. Struct. 1283 (2023) 1385279.
[19] X. Min, S. Guo, Y. Lu, X. Xu, Investigation on the inhibition mechanism and binding behavior of cryptolepine to α-glucosidase and its hypoglycemic activity by multi- spectroscopic method, J. Lumin. 269 (2024) 120437.
[20] X. Zhang, Y.-Y. Zheng, C.-M. Hu, X.-Z. Wu, J. Lin, Z. Xiong, K. Zhang, X.-T. Xu, Synthesis and biological evaluation of coumarin derivatives containing oxime ester as α-glucosidase inhibitors, Arab. J. Chem. 15 (2022) 104072.
[21] X.-Z. Wu, W.-J. Zhu, L. Lu, C.-M. Hu, Y.-Y. Zheng, X. Zhang, J. Lin, J.-Y. Wu, Z. Xiong, K. Zhang, X.-T. Xu, Synthesis and anti-α-glucosidase activity evaluation of betulinic acid derivatives, Arab. J. Chem. 16 (2023) 104659.
[22] A.M. Dirir, M. Daou, A.F. Yousef, L.F. Yousef, A review of alpha-glucosidase inhibitors from plants as potential candidates for the treatment of type-2 diabetes, Phytochem Rev 21 (2022) 1049–1079.

[23] X. Li, Y. Bai, Z. Jin, B. Svensson, Food-derived non-phenolic α-amylase and α-glucosidase inhibitors for controlling starch digestion rate and guiding diabetes-friendly recipes, LWT 153 (2022) 112455.
[24] Y.Y. Guo, J.Y. Zhang, J.F. Sun, H. Gao, A comprehensive review of small- molecule drugs for the treatment of type 2 diabetes mellitus: synthetic approaches and clinical applications, Eur. J. Med. Chem. 5 (2024) 116185.
[25] J. Brahmi, S. Ghannay, S. Bakari, A. Kadri, K. Aouadi, M. Msaddek, S. Vidal, Unprecedented stereoselective synthesis of 3-methylisoxazolidine-5-aryl-1,2,4-oxadiazoles via 1,3-dipolar cycloaddition and study of their *in vitro* antioxidant activity, Synth. Commun. 46 (2016) 2037–2044.
[26] A. Al-Adhreai, M. Alsaeedy, A. Alrabie, I. Al-Qadsy, S. Dawbaa, Z.M. Alaizeri, H.A. Alhadlaq, A. Al-Kubati, M. Ahamed, M. Farooqui, Design and synthesis of novel enantiopure Bis(5-Isoxazolidine) derivatives: insights into their antioxidant and antimicrobial potential via *in silico* drug-likeness, pharmacokinetic, medicinal chemistry properties, and molecular docking studies, Heliyon 8 (2022) e09746.
[27] S. Ghannay, S. Bakari, A. Ghabi, A. Kadri, M. Msaddek, K. Aouadi, Stereoselective synthesis of enantiopure N-substituted pyrrolidin-2,5-dione derivatives by 1,3-dipolar cycloaddition and assessment of their *in vitro* antioxidant and antibacterial activities, Bioorg. Med. Chem. Lett. 27 (2017) 2302–2307.
[28] M. Hossain, I. Habib, K. Singha, A. Kumar, FDA-approved heterocyclic molecules for cancer treatment: synthesis, dosage, mechanism of action and their adverse effect, Heliyon 10 (2024) E23172.
[29] J. Brahmi, S. Bakari, S. Nasri, H. Nasri, A. Kadri, K. Aouadi, Synthesis and SPAR exploration of new semicarbazone-triazole hybrids in search of potent antioxidant, antibacterial and antifungal agents, Mol. Biol. Rep. 46 (2019) 679–686.
[30] S. Ghannay, M. Snoussi, S. Messaoudi, A. Kadri, K. Aouadi, Novel enantiopure isoxazolidine and C-alkyl imine oxide derivatives as potential hypoglycemic agents: design, synthesis, dual inhibitors of α-amylase and α-glucosidase, ADMET and molecular docking study, Bioorg. Chem. 104 (2020) 104270.
[31] Z. Ali, W. Rehman, L. Rasheed, A.Y. Alzahrani, N. Ali, R. Hussain, A.H. Emwas, M. Jaremko, M.H. Abdellattif, New 1,3,4-thiadiazole derivatives as α-glucosidase inhibitors: design, synthesis, DFT, ADME, and *in vitro* enzymatic studies, ACS Omega 9 (2024) 7480–7490.
[32] S.A. Ullah, A. Saeed, M. Azeem, M.B. Haider, M.F. Erben, Exploring the latest trends in chemistry, structure, coordination, and diverse applications of 1-acyl-3-substituted thioureas: a comprehensive review, RSC Adv. 14 (2024) 18011–18063.
[33] E.U. Mughal, M.B. Hawsawi, N. Naeem, A. Hassan, M.S. Alluhaibi, S.W. Ali Shah, Y. Nazir, A. Sadiq, H.A. Alrafai, S.A. Ahmed, Exploring fluorine- substituted piperidines as potential therapeutics for diabetes mellitus and Alzheimer's diseases, Eur. J. Med. Chem. 273 (2024) 116523.
[34] H. Zahid, M. Abid, S. Qasim, I. Aqeel, U.M. Ehsan, K. Wajiha, B. Ayesha, I. Jamshed, M. Amara, Synthesis and evaluation of amide and thiourea derivatives as carbonic anhydrase (CA) inhibitors, ACS Omega 7 (2022) 47251–47264.
[35] R. Ronchetti, G. Moroni, A. Carotti, A. Gioiello, E. Camaioni, Recent advances in urea- and thiourea-containing compounds: focus on innovative approaches in medicinal chemistry and organic synthesis, RSC Med. Chem. 12 (2021) 1046–1064.
[36] J.E. Mendieta-Wejebe, M.C. Rosales-Hernández, I.I. Padilla-Martínez, E.V. García-Báez, A. Cruz, Design, synthesis and biological activities of (Thio)Urea benzothiazole derivatives, Int. J. Mol. Sci. 24 (2023) 9488.
[37] Ş.D. Doğan, M.G. Gündüz, H. Doğan, V.S. Krishna, C. Lherbet, D. Sriram, Design and synthesis of thiourea-based derivatives as Mycobacterium tuberculosis growth and enoyl acyl carrier protein reductase (InhA) inhibitors, Eur. J. Med. Chem. 199 (2020) 112402.
[38] C. Efeoglu, D. Yetkin, Y. Nural, A. Ece, Z. Seferoğlu, F. Ayaz, Novel urea- thiourea hybrids bearing 1,4-naphthoquinone moiety: anti-inflammatory activity on mammalian macrophages by regulating intracellular PI3K pathway, and molecular docking study, J. Mol. Struct. 1264 (2022) 133284.
[39] A.K. Ghosh, M. Brindisi, Urea derivatives in modern drug discovery and medicinal chemistry, J. Med. Chem. 63 (2020) 2751–2788.
[40] S.K. Sahoo, O. Ommi, S. Maddipatla, et al., Isoxazole carboxylic acid methyl ester-based urea and thiourea derivatives as promising antitubercular agents, Mol. Divers. 27 (2023) 2037–2052.
[41] J.M. Hubbard, M.R. Mahoney, W.S. Loui, L.R. Roberts, T.C. Smyrk, Z. Gatalica, M. Borad, S. Kumar, S.R. Alberts, Phase I/II randomized trial of Sorafenib and bevacizumab as first-line therapy in patients with locally advanced or metastatic hepatocellular carcinoma: north central cancer treatment group trial N0745 (alliance), Target Oncol 12 (2017) 201–209.
[42] R. Verrijk, I. Smolders, R. Huiskamp, et al., Pharmacokinetics in melanoma- bearing mice of 5-dihydroxyboryl-6-propyl-2-thiouracil (BPTU), a candidate compound for boron neutron capture therapy, Br. J. Cancer 69 (1994) 641–647.
[43] Z.G. Gao, K.A. Jacobson, Distinct signaling patterns of allosteric antagonism at the P2Y1 receptor, Mol. Pharmacol. 92 (2017) 613–626.
[44] B.K. Singh, M. Singha, S. Basak, R. Biswas, A.K. Das, A. Basak, Fluorescently labelled thioacetazone for detecting the interaction with Mycobacterium dehydratases HadAB and HadBC, Org. Biomol. Chem. 20 (2022) 1444–1452.
[45] A.T. Black, Chapter 12 - dermatological drugs, topical agents, and cosmetics, in: Sidhartha D. Ray (Ed.), Side Effects of Drugs Annual, vol. 39, Elsevier, 2017, pp. 145–155.
[46] https://www.fda.gov/drugs/resources-information-approved-drugs/fda-approves-enzalutamide-non-metastatic-castration-sensitive-prostate-cancer-biochemical-recurrence.
[47] Ş. Erol Günal, Synthesis of 2-fluorobenzoyl thiourea derivatives, İstanbul Ticaret Üniversitesi Fen Bilimleri Dergisi 22 (2023) 417–424.
[48] K. Sawami, A. Tanaka, K. Node, Glimepiride: an old antidiabetic medication with potential as a new cardiovascular therapeutic? Eur. J. Prev. Cardiol. 30 (2023) e46–e47.
[49] D.M. Liu, C. Dong, R.T. Ma, A colorimetric method for screening α-glucosidase inhibitors from flavonoids using 3,3',5,5'-tetramethylbenzidine as a chromogenic probe, Colloids Surf. B Biointerfaces 197 (2021) 111400.
[50] M. Taibi, A. Elbouzidi, M. Haddou, A. Baraich, H. Loukili, T. Moubchir, A. Allali, A. khoulati, R. Bellaouchi, A. Asehraou, M. Addi, A.M. Salamatullah, M. Bourhia, F. Siddique, B. El Guerrouj, K. Chaabane, Phytochemical characterization and multifaceted bioactivity assessment of essential oil from Ptychotis verticillata Duby: anti-diabetic, anti-tyrosinase, and anti-inflammatory activity, Helyion 10 (2024) E29459.
[51] A. Busili, K. Kumar, L. Kudrna, I. Busaily, The risk factors for mental health disorders in patients with type 2 diabetes: an umbrella review of systematic reviews with and without meta-analysis, Heliyon 10 (2024) E28782.
[52] M. Zhao, K. Wang, R. Lin, F. Mu, J. Cui, X. Tao, Y. Weng, J. Wang, Influence of glutamine metabolism on diabetes Development: a scientometric review, Helyion 10 (2024) E25258.
[53] S. Abdullah, A. Iqbal, A.K. Ashok, F.C. Kaouche, M. Aslam, S. Hussain, J. Rahman, M.M. Hayat, M. Ashraf, Anti-enzymatic and DNA docking studies of montelukast: a multifaceted molecular scaffold with *in vitro* investigations, molecular expression analysis and molecular dynamics simulations, Heliyon 10 (2024) E24470.
[54] F. Alhawday, F. Alminderej, S. Ghannay, B. Hammami, A.E.A.E. Albadri, A. Kadri, K. Aouadi, *In silico* design, synthesis, and evaluation of novel enantiopure isoxazolidines as promising dual inhibitors of α-amylase and α- glucosidase, Molecules 29 (2024) 305.
[55] N. Bouali, M.B. Hammouda, I. Ahmad, S. Ghannay, A. Thouri, A. Dbeibia, H. Patel, W.S. Hamadou, K. Hosni, M. Snoussi, et al., Multifunctional derivatives of spiropyrrolidine tethered indeno-quinoxaline heterocyclic hybrids as potent antimicrobial, antioxidant and antidiabetic agents: design, synthesis, *in vitro* and *in silico* approaches, Molecules 27 (2022) 7248.
[56] A. Ghabi, J. Brahmi, F. Alminderej, S. Messaoudi, S. Vidald, A. Kadri, K. Aouadi, Multifunctional isoxazolidine derivatives as α-amylase and α-glucosidase inhibitors, Bioorg. Chem. 98 (2020) 103713.
[57] F. Alminderej, S. Ghannay, M.O. Elsamani, F. Alhawday, A.E.A.E. Albadri, S.E.I. Elbehairi, M.Y. Alfaifi, A. Kadri, K. Aouadi, *In vitro* and in silico evaluation of antiproliferative activity of new isoxazolidine derivatives targeting EGFR: design, synthesis, cell cycle analysis, and apoptotic inducers, Pharmaceuticals 16 (2023) 1025.
[58] I.M.M. Othman, M.A.M. Gad-Elkareem, E.H. Anouar, M. Snoussi, K. Aouadi, A. Kadri, Novel fused pyridine derivatives containing pyrimidine moiety as prospective tyrosyl-tRNA synthetase inhibitors: design, synthesis, pharmacokinetics and molecular docking studies, J. Mol. Struct. 1219 (2020) 128651.
[59] I.M.M. Othman, M.A.M. Gad-Elkareem, E.H. Anouar, K. Aouadi, A. Kadri, M. Snoussi, Design, synthesis ADMET and molecular docking of new imidazo[4,5- b] pyridine-5-thione derivatives as potential tyrosyl-tRNA synthetase inhibitors, Bioorg. Chem. 102 (2020) 104105.

[60] H.A. Radwan, I. Ahmad, I.M.M. Othman, M.A.M. Gad-Elkareem, H. Patel, K. Aouadi, M. Snoussi, A. Kadri, Design, synthesis, *in vitro* anticancer and antimicrobial evaluation, SAR analysis, molecular docking and dynamic simulation of new pyrazoles, triazoles and pyridazines based isoxazole, J. Mol. Struct. 1264 (2022) 133312.
[61] M.I.H. El-Qaliei, S.A.S. Mousa, M.H. Mahross, A.M.A. Hassane, M.A.M. Gad-Elkareem, H. Anouar, M. Snoussi, K. Aouadi, A. Kadri, Novel (2-Oxoindolin- 3-ylidene)methyl)-1H-pyrazole and their fused derivatives: design, synthesis, antimicrobial evaluation, DFT, chemical approach, *in silico* ADME and molecular docking studies, J. Mol. Struct. 1264 (2022) 133299.
[62] I.M.M. Othman, M.A.M. Gad-Elkareem, H.A. Radwan, R. Badraoui, K. Aouadi, M. Snoussi, A. Kadri, Synthesis, structure-activity relationship and *in silico* studies of novel pyrazolothiazole and thiazolopyridine derivatives as prospective antimicrobial and anticancer agents, ChemistrySelect 6 (2021) 7860–7872.
[63] R. Badraoui, T. Rebai, S. Elkahoui, M. Alreshidi, V. N. Veettil, E. Noumi, K. A. Al- Motair, K. Aouadi, A. Kadri, V. De Feo, et al., Allium subhirsutum L. As a potential source of antioxidant and anticancer bioactive molecules: HR-LCMS phytochemical profiling, *in vitro* and *in vivo* pharmacological study, Antioxidants 9 (2020) 1003.
[64] S. Ghannay, A. Kadri, K. Aouadi, Synthesis, *in vitro* antimicrobial assessment, and computational investigation of pharmacokinetic and bioactivity properties of novel trifluoromethylated compounds using *in silico* ADME and toxicity prediction tools, Monatsh. Chem. 151 (2020) 267–280.
[65] I.M.M. Othman, M.A.M. Gad-Elkareem, E.H. Anouar, K. Aouadi, M. Snoussi, A. Kadri, New substituted pyrazolones and dipyrazolotriazines as promising tyrosyl-tRNA synthetase and peroxiredoxin-5 inhibitors: design, synthesis, molecular docking and structure-activity relationship (SAR) analysis, Bioorg. Chem. 109 (2021) 104704.
[66] F.Z. Thari, S. Fettach, E.H. Anouar, H. Tachallait, H. Albalwi, Y. Ramli, J.T. Mague, K. Karrouchi, M.E.A. Faouzi, K. Bougrin, Synthesis, crystal structures, α-glucosidase and α-amylase inhibition, DFT and molecular docking investigations of two thiazolidine-2,4-dione derivatives, J. Mol. Struct. 1261 (2022) 132960.
[67] D. Shahzad, A. Saeed, F.A. Larik, P.A. Channar, Q. Abbas, M.F. Alajmi, M.I. Arshad, M.F. Erben, M. Hassan, H. Raza, S.Y. Seo, H.R. El-Seedi, Novel C-2 symmetric molecules as α-glucosidase and α-amylase inhibitors: design, synthesis, kinetic evaluation, molecular docking and pharmacokinetics, Molecules 24 (2019) 1511.
[68] V. Nahoum, G. Roux, V. Anton, P. Rougé, A. Puigserver, H. Bischoff, B. Henrissat, F. Payan, Crystal structures of human pancreatic α-amylase in complex with carbohydrate and proteinaceous inhibitors, Biochem. J. 346 (2000) 201–208.
[69] M. Fan, Q. Feng, M. He, W. Yang, Z. Peng, Y. Huang, G. Wang, Synthesis, α-glucosidase inhibition and molecular docking studies of natural product 2-(2-phenyethyl)chromone analogues, Arab. J. Chem. 15 (2022) 104301.
[70] X.T. Xu, X.Y. Deng, J. Chen, Q.M. Liang, K. Zhang, D.L. Li, P.P. Wu, X. Zheng, R.P. Zhou, Z.Y. Jiang, A.J. Ma, W.H. Chen, S.H. Wang, Synthesis and biological evaluation of coumarin derivatives as alpha-glucosidase inhibitors, Eur. J. Med. Chem. 189 (2020) 112013.